

Multi-Wavelength Study of Sgr A* in the Galactic Centre

Santanu Ganguly

Liverpool John Moores University

Contents

| | |
|---|----|
| Abstract | 3 |
| Multi-Wavelength Study of Sgr A* in the Galactic Centre | 3 |
| Sgr A* : Variability in the NIR, X-ray and Radio | 6 |
| Variability in NIR..... | 7 |
| Variability in X-Ray | 11 |
| Coordinated X-Ray/NIR Study of Sgr A* | 12 |
| Variability of Sgr A* in Sub-mm and Radio | 14 |
| Submm-VLBI of Sgr A* with EHT- Shadow of a Black Hole..... | 16 |
| Conclusion | 20 |
| References:..... | 21 |

Abstract

Sgr A* is a bright and compact source of radio, sub-mm, Near-Infra-Red (NIR), submm-VLBI and X-rays at the center of the Milky Way and has been imaged with great precision using various telescopes and instruments. Detailed observations with radio telescopes and additional observations in multiple wavelengths from various space-based telescopes have captured detailed images of the environment around Sgr A*, revealing the accretion disk of material that is trapped by the central black hole's immense gravity. The material swirls around before falling into the black hole, causing it to be heated to millions of degrees through friction forces, while emitting brightly across the whole electromagnetic spectrum and producing very high-energy cosmic rays in the process. This review of recent literature focusses on variability of Sgr A* in NIR, X-rays, Radio and submm-Very Long Baseline Interferometry (VLBI) with EHT (Event Horizon Telescope).

Keywords: Sgr A*, sub-mm, VLBI, X-ray, NIR, EHT

Multi-Wavelength Study of Sgr A* in the Galactic Centre

Sagittarius A* (Sgr A*), discovered in 1974, is a radio source at the center of our own Galaxy. It lies in the direction of Sagittarius, around R.A. 17h 46m and Dec. $-28^{\circ} 56'$. The nucleus of the Milky Way contains a complex of gas, dust, stars, supernova remnants, magnetic filaments, and, almost certainly, a massive black hole at the very centre. There are two main populations of black holes that have been discovered: (i) stellar-mass black holes with masses in the range $5M_{\odot}$ to $30M_{\odot}$, millions of which are present in each galaxy in the universe, and (ii) supermassive black holes with masses in the range 10^6M_{\odot} to $10^{10}M_{\odot}$, one each in the nucleus of every

galaxy. There is strong evidence that all these objects are true black holes with event horizons. Majority of these black holes have very low accretion luminosities and hence, are very dim. In the absence of the glare of a bright central source, it is possible to carry out high resolution imaging and spectroscopic observations relatively close to the black hole and thereby estimate the black hole mass via dynamical methods.

Various groups over last two decades, have successfully used the largest telescopes on Earth to obtain diffraction-limited infrared images of the Galactic Center, and have mapped the trajectories of stars orbiting the Galactic nucleus. All the stars move on Keplerian orbits around a common focus [Russell et al., 2013; Ghez et al., 2005a] (see Fig. 1.1) containing a dark mass of $4.4 \pm 0.4 \times 10^6 M_{\odot}$ [Meyer & Ghez et al., 2012]. It is estimated from theory (for e.g., “Gravitation”, Wheeler, Thorne et al.) that since the dark mass must be interior to the pericenter of the most compact stellar orbit, its radius must be $< 10^3 R_g$, where R_g is the gravitational radius of a black hole.

Zajaček et. al (2017) did a continuum analysis of NIR polarimetry data combined with the radiative transfer modelling of the Dusty S-cluster Object (DSO/G2) orbiting Sgr A* in the Galactic centre in order to constrain the nature and the geometry of the DSO. Their composite model of the DSO – a dust-enshrouded star that consists of a stellar source, dusty and optically thick - shows that the DSO is a peculiar source of compact nature in the S cluster.

The luminosity of Sgr A* is thought to be due to partial capture of thermal winds from a neighboring cluster of massive stars. But, the bolometric luminosity of Sgr A* ($\sim 100 L_{\odot}$) is several orders of magnitude lower than expected for the estimated accretion rate. The broad-band spectrum of Sgr A* peaks at sub-millimeter wavelengths, which is the dividing line between optically thin infrared and optically thick millimeter and radio emission. The existence of flare emission from Sgr A* is now well established in both optically thick and thin regimes.

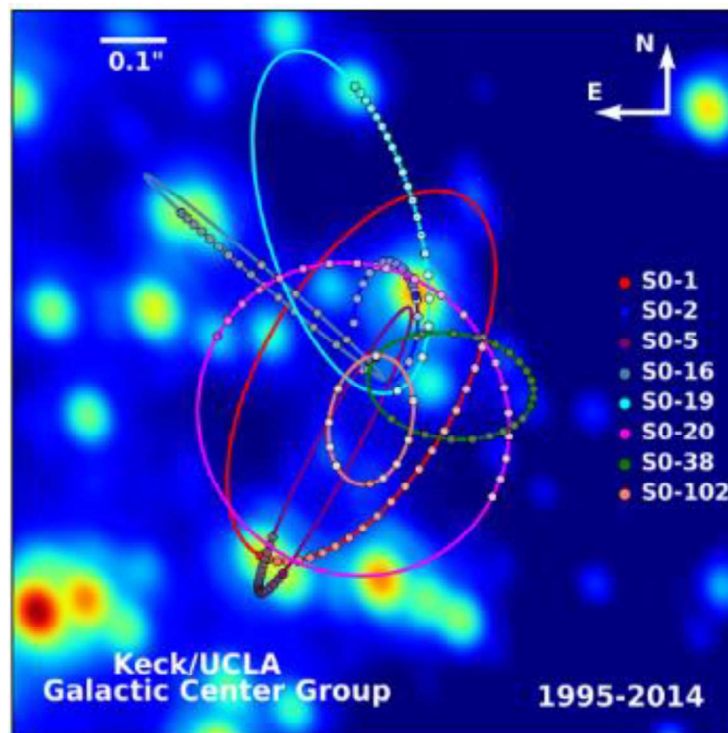


Figure 1.1 Orbital tracks on the plane of the sky over the period 1995-2014 of 8 bright stars (S0-1, S0-2, ... , S0-102) at the center of our Galaxy. Keplerian fits to these orbits give the position and mass of the supermassive black hole in the nucleus of the Galaxy. (Figure courtesy of Andrea Ghez and her research team at UCLA, based on data obtained with the W. M. Keck Telescopes: <http://www.galacticcenter.astro.ucla.edu/about.html>)

Sgr A* has been shown to be largely at rest with respect to the Galaxy, moving with a speed less than about 1 km s^{-1} [Reid et al., 2004]. The velocities of stars orbiting in its vicinity are quite large, the fastest stars move with speeds up to 10^4 km s^{-1} . Consequently, from theoretical point-

of-view, this implies that Sgr A* must be more massive than $10^5 M_{\odot}$. The only plausible interpretation is that Sgr A* is identical to the $4.4 \times 10^6 M_{\odot}$ object inferred from stellar orbits.

Sgr A* is a bright and compact source of radio, sub-*mm*, Near-Infra-Red (NIR) and X-rays at the center of the Milky Way and has been imaged with great precision using interferometric techniques. Recent observations indicate that emission at 1.3 mm wavelength comes from within a radius of a few R_g [Doeleman et al., 2008; Fish et al., 2011]. This restrictive size constraint makes it almost certain that Sgr A* must be a supermassive black hole. Because of cool interstellar dust along the line of sight, the Galactic Centre cannot be studied at visible, ultraviolet or soft X-ray wavelengths. The available information about the Galactic Center comes from observations at gamma ray, hard X-ray, infrared, sub-mm and radio wavelengths.

Sgr A* : Variability in the NIR, X-ray and Radio

A number of telescopes have been coordinated to observe Sgr A* simultaneously in order to understand the correlation and the radiation mechanism of flare emission in different wavelength bands, for example the short time scale variability of emission from Sgr A* in near-IR, X-ray and radio wavelengths. Yusef-Zadeh et al. (2010) report minute time scale variability at 7 and 13 mm placing a strong constraint on the nature of the variable emission. The hourly time scale variability has been modeled as follows: as the peak frequency of emission shifts toward lower frequencies as a self-absorbed synchrotron source expands adiabatically near the acceleration site. The short time scale variability, on the other hand, indicates a strong constraint on the size of the emitting region. Assuming that rapid minute time scale fluctuations of the emission is optically thick in radio wavelength, light travel reasoning requires relativistic particle energy,

thus suggesting the presence of outflow from Sgr A*.

Variability in NIR

Near-infrared observations of the center of the Milky Way were greatly aided by advent of adaptive optics instrumentation on 8-10 m-class telescopes. Since circa 2000 high-resolution NIR imaging with speckle interferometry and adaptive optics have led to the first clear evidence that the gravitational potential in the central parsec of the Milky Way is dominated by a point mass (e.g., Eckart & Genzel, 1996; Ghez et al., 1998). Continued observations revealed the first detection of stellar acceleration near Sgr A* (Ghez et al., 2000; Eckart et al., 2002).

The central arcsecond of the Galaxy contains a stellar population of several OB stars which orbit the black hole on relaxed orbits. Current theories suggest that these stars could not have been formed on their current orbit, for the tidal forces prevent star formation that close to Sgr A*. However, they are quite young, and the mechanism of their migration from their nursery to their current location is not well understood and is referred to as the “paradox of youth” (Ghez et al., 2003). One of the very well-known of these “S” stars is S2 or S0-2 (SIMBAD: “[EG97] S2” and “[GKM98] S0-2”) which has been observed for more than one of its 15.2-year orbits, passing periapsis at about 1% of the speed of light.

The intensity of Sgr A* shows spontaneous flux density outbursts at radio to X-ray frequencies, commonly referred to as flares (Mauerhan et al. 2005; Marrone et al. 2006; Yusef-Zadeh et al. 2008; Eckart et al. 2008a,b,c, 2009, 2012; Lu et al. 2011; Miyazaki et al. 2012). These intensity

irregularities appear on timescales ranging from 1-2 hours (main flares) down to 7-10 minutes (sub-flares) (Eckart et al. 2006a) with stronger activity at shorter wavelengths (Baganoff et al. 2001; Genzel et al. 2003; Ghez 2004; Eckart et al. 2006b,c). The short timescales suggest that this feature originates in a very compact region, possibly located close to the event horizon of the BH. The first trial of the detection of flux by UCLA and MPE groups in 2002 yielded an ambiguous result. This was due to the fact that the closest approach of the bright short-period star S2 blended the two sources producing imprecise data measurement. However, repeat measurements about a year later when S2 was appropriately far away, clearly showed a variable red source at the center of the galaxy (Genzel et al. 2003; Ghez et al. 2004, figure 1.2).

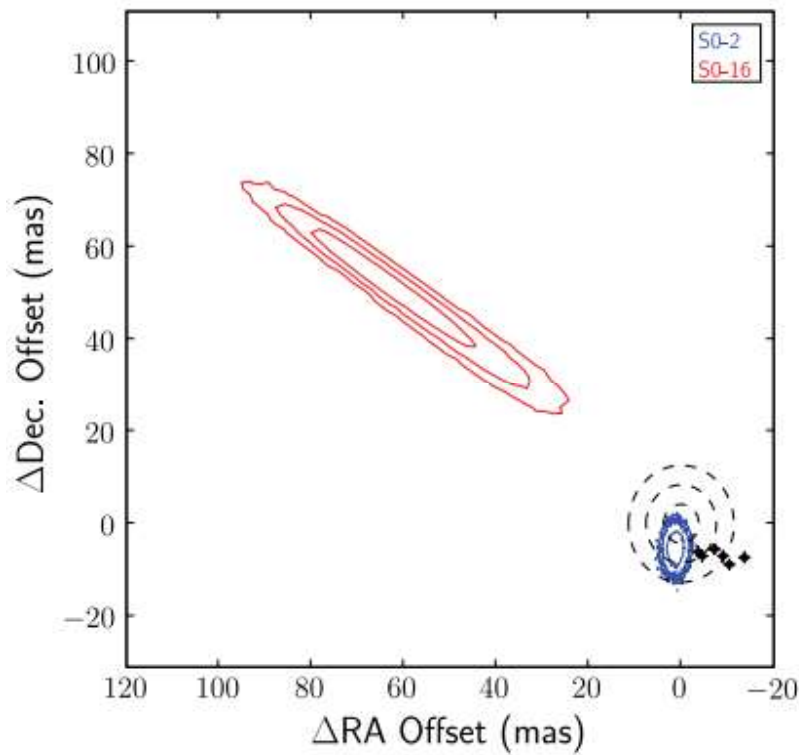


Figure 1.2 Comparison of estimates of the black hole's location. Colored contours represent the estimates of the dynamical center from model fits to kinematic measurements of S2 ($K=14.0$; blue) and S16 ($K=15.0$; red). Black contours show the Sgr A* radio position. All contours are plotted at the 68%, 95%, and 99.7% confidence levels. The discrepancy in the black hole's location from S0-16's positional measurements appear to be a consequence of biases from unrecognized, underlying

stars and thus only S0-2's measurements are used to infer the properties of the central black hole. Adapted from Ghez et al. (2008)

The strong NIR flaring of Sgr A* is somewhat explained by the external material from the outer disk raining down on the inner disk, producing transient outbursts, as seen in NIR and X-ray wavelengths. Studies (Eckart et al. 2006b; Meyer et al. 2006a,b, 2007; Zamaninasab et al. 2010) show that polarimetric observations of Sgr A*'s flux excursions are consistent with a “hot spot” model where the emission from a bright region of the accretion flow is aided by strong gravitational lensing.

Meyer et al. (2008) modeled the intrinsic NIR variability of Sgr A* as a purely random process and showed this for the longest continuous light curve observed so far (600 *min.*).

Meyer et al. (2009) found a power-law break in the NIR PSD of the galactic center BH (figure 1.3). They found the timescale in Sgr A* to be in agreement with a proposed scaling relation that uses bolometric luminosity and black hole mass as parameters (McHardy et al. 2006) where the result fits the expected value *if only* linear scaling with black hole mass is assumed. Based on this, they argue that the accretion process is the same for small and large BHs. The authors suggest that the luminosity-mass-timescale relation applies only to black hole systems in the soft state, while in the hard state, which is characterized by lower luminosities and accretion rates, there seems to be linear mass scaling, linking Sgr A* to hard-state stellar mass black holes.

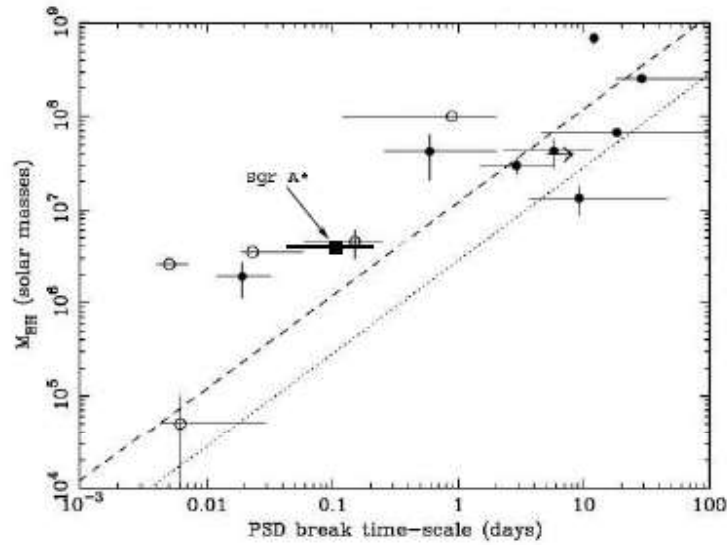


Figure 1.3 Break timescale of Sgr A* as reported by Meyer et al. (2009) over plotted onto figure 11 of Uttley & McHardy (2005), which shows BH mass versus PSD break timescale for various AGN. The mass of Sgr A* has been taken from Ghez et al. (2008). Its uncertainty corresponds to the height of the black square. Filled circles mark masses determined from optical reverberation mapping, open circles represent masses determined using other methods. The straight lines represent the expected relations if linear mass scaling is assumed from the typical timescales observed in the high/soft (dashed line) and low/hard (dotted line) state of the BHXRB Cyg X-1 (assuming $10 M_{\odot}$ for its mass). From Meyer et al. (2009).

Variability of the NIR emission of Sgr A* is a key carrier of information regarding the dynamics of the accretion flow. Short (\sim minutes) time scales probe the transient acceleration of particles associated with the dissipation of kinetic and magnetic energy on small scales within the accretion flow. Intermediate time scales (hours) probe the dynamical evolution of the accretion flow on a timescale of a few orbits, as in the theoretical study of Chan et al. (2009). Longer time scales (days to months) probe the crucial and unexplored dynamics of the stochastic feeding of the inner accretion flow from larger radii and the draining of the inner flow onto the black hole. Future variability measurements of Sgr A* are expected to show the low-level accretion flow that produces quiescent flux variations of a factor of 2 whereas the flaring activity from transient

events is expected to show flux variations of about a factor ten.

Rauch et. al (2015) observed the radio source Sgr A* at 7 mm in the context of a NIR triggered global Very Long Baseline Array (VLBA) campaign. An observed NIR flare on May 17 was followed ~ 4.5 hours later by an increase in flux density of 0.22 Jy at 43 GHz. The authors state that this agrees well with the expected time delay of events that are casually connected by adiabatic expansion.

Variability in X-Ray

Sgr A* is a very weak X-ray and NIR source (see, e.g., Melia & Falcke 2001). High resolution imaging at the corresponding wavelengths by s Chandra (X-rays) and NAOS/CONICA at the ESO VLT (NIR) reveal the emission from Sgr A* to be highly variable at these wavelengths. Weak X-ray counterpart to Sgr A* was discovered in 1999.

Baganoff et al. (2001) reported a large X-ray outburst lasting almost 3 hours and having a peak intensity of 36 times the quiescent level. Studies of X-ray flares observed by both Chandra and XMM-Newton. The variability in their time scales and studies of their structure on several-minute time scales during the flares, indicate that they arise much closer to the black hole than the quiescent emission, likely within a few tens of *Schwarzschild radii*. The reported rate of detectable flares is about once per day. Since flares are point sources, the undetected ones could also lead to a narrowing of the perceived size of the quiescent emission region. Significantly

bright flares have been detected from Sgr A*: two by XMM (Porquet et al. 2003, 2008) and one by Chandra/HETG (Nowak et al. 2012), all demonstrating peak fluxes in the order of 100 times the quiescent level.

Unlike near-IR structure function plots that can be fit by single power laws, radio and X-ray structure function plots are fit by multiple power laws in different time lag domains. Structure function analysis of the data found in near-IR, X-ray and radio data suggest that most of the power falls in the long time scale fluctuation of the emission from Sgr A*.

Coordinated X-Ray/NIR Study of Sgr A*

Unlike near-IR structure function plots that can be fit by single power laws, radio and X-ray structure function plots are fit by multiple power laws in different time lag domains. Structure function analysis of the data found in near-IR, X-ray and radio data suggest that most of the power falls in the long time scale fluctuation of the emission from Sgr A*.

The first successful simultaneous near-infrared and X-ray detection of the Sgr A* counterpart, was carried out using the NACO adaptive optics (AO) instrument at the European Southern Observatory's Very Large Telescope and the ACIS-I instrument aboard the *Chandra X-ray Observatory* (Eckart et al., 2004). A flare was detected at X-rays that was covered simultaneously in its decaying part by the NIR observations (Figure 1.4). Eckart et al. (2004) stated that the flaring state can be explained with a synchrotron self-Compton (SSC) model involving up-scattered sub-millimeter photons from a compact source component, possibly with modest bulk relativistic motion. The size of that component is assumed to be of the order of a

few times the Schwarzschild radius. A conservative estimate of the upper limit of the time lag between the ends of the NIR and X-ray flares is of the order of 15 minutes. The simultaneity of the flares at NIR/X-ray also confirms clearly that the X-ray source seen by *Chandra* is indeed associated with Sgr A*.

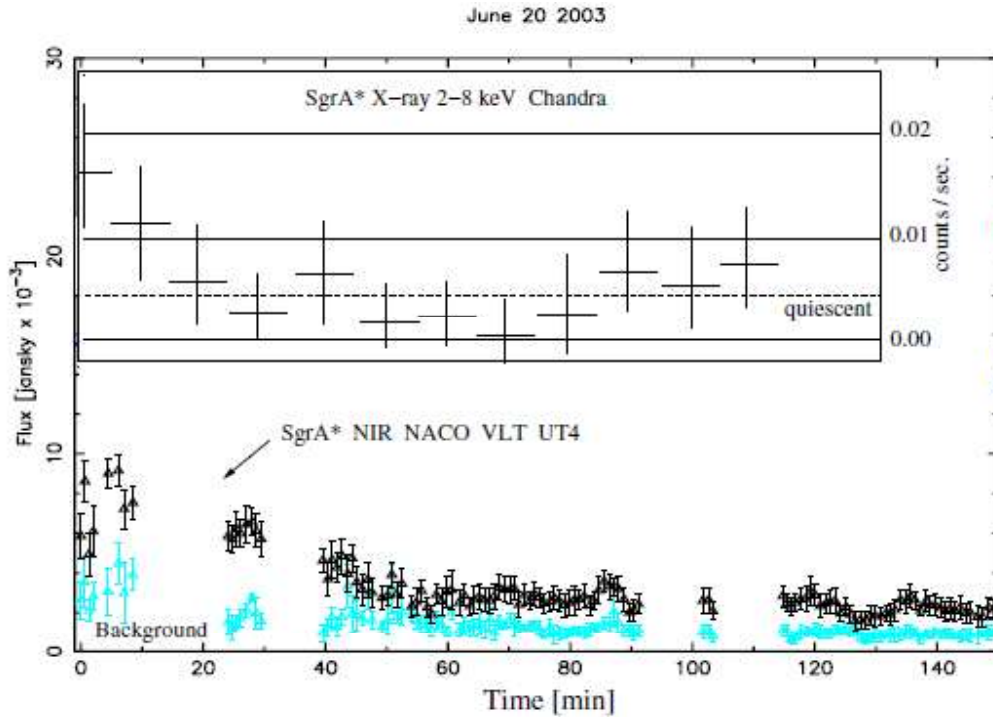


Figure 1.4 Sgr A* flare observed simultaneously at NIR/X-ray wavelengths (Eckart et al., 2004). The X-ray and NIR light curves are plotted with a common time axis. Straight solid lines in the inserted box represent the 0.00, 0.01, and 0.02 counts per second levels. The straight dashed line represents the X-ray quiescent-state flux density level. The NIR observations started on 19 June 2003 at 23:51:15 (AT), 0.38 minutes before the midpoint of the highest X-ray measurement. From Eckart et.al (2004)

X-ray flares, during which the emission from Sgr A* rises by factors of a few tens up to one hundred, were first detected by Baganoff et al. (2001). NIR flares were detected by Genzel et al. (2003) and Ghez et al. (2004). During NIR flares the emission from Sgr A* increases by a factor of a few in this wavelength regime. Both at X-ray and NIR wavelengths the flares show

variability on time scales of just a few minutes. This points to very compact source regions of not more than a few tens of Schwarzschild radii in size.

Simultaneous X-ray and IR observations has shown that every X-ray flare corresponds reasonably well in time with a well-defined and relatively bright maximum in the infrared light curve (Eckart et al. 2004; Ghez et al. 2004; Marrone et al. 2008; Dodds-Eden et al. 2009; Eckart et al. 2012). The reverse is not true: only a fraction of the IR maxima correspond with an X-ray flare.

Variability of Sgr A* in Sub-mm and Radio

Ground based radio-observations are limited to a range of wavelengths that can go through the Earth atmosphere - 1mm – 10m (or 30 – 300 GHz). At longer wavelengths (lower frequencies), transmission is limited by the ionosphere, which reflects waves with frequencies less than 30GHz, while at higher frequencies (at millimeter range), radio signals are prone to atmospheric absorption. In order to observe faint sources with good angular resolution, radio telescopes need to be i) extremely large and ii) be placed in very high and dry sites, e.g. ALMA, VLA, etc.

The VLA images of Galactic Centre rendered at 6 cm show more detail, including 3 spiral arms 3 light-years long. The image taken at 2 cm shows the central 2 light year region, features spiral pattern of Sagittarius A West and the point-like source of radio emission known as Sagittarius A* (Figure 1.5).

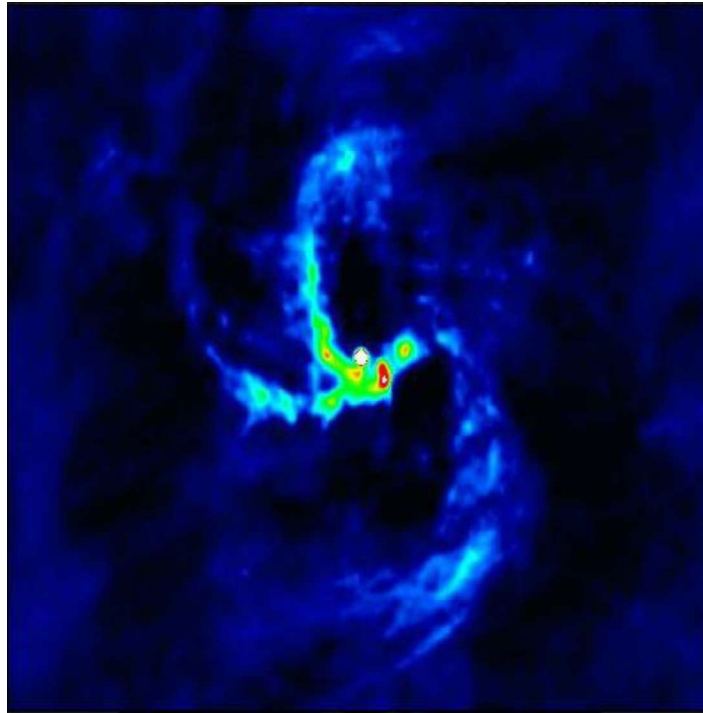


Figure 1.5 Radio continuum emission at 3.6 cm from the inner few parsecs of our Galaxy. The bright point source in the center is Sagittarius A. The mini-spiral of emission around the point source is from ionized gas that is in systematic motion about Sgr A*. Image courtesy of NRAO/AUI

Radio observations at 7 mm and 3.5 mm have detected intrinsic structure in Sgr A*, but the spatial resolution of observations at these wavelengths is limited by interstellar scattering. The apparent size of Sgr A* is dominated by scatter broadening at frequencies up to 50 GHz and the smallest size detected (Doeleman et al., 2008) is $\sim 0.1 AU$ at $\sim 1.3 mm$. This is less than the expected apparent size of the event horizon (as observed from 8 kpc), suggesting that most of SgrA* emission may not be centered on the black hole, but arises in the surrounding accretion flow. Interferometric study at a wavelength of 3 mm by Marrone et al. (2006) indicate that intrinsic radio variability of Sgr A* is best seen on time scales of hours.

Indications of the nature of the emitting region can be obtained by comparing the light curves of Sgr A* at different wavelengths. Yusef-Zadeh et al. (2006b) carried out a VLA study between frequencies of 22 and 43 GHz and showed a delay of the 22 GHz light curve, relative to that at 43 GHz, by 20 to 40 min. Yusef-Zadeh et al. (2008) coupled the same two frequencies with a simultaneous (sub-mm) 350 GHz observation and a Chandra observation showing an X-ray flare, and found that the X-ray flare precedes the sub-mm flare by about 90 min, as the expanding plasmon model would qualitatively predict, and again that the 22 GHz emission lags the 43 GHz emission.

The expanding blob model of van der Laan (1966) predicts that X-ray and near-IR emission peaks should occur simultaneously, since they are both optically thin throughout the expansion. This is consistent with almost all observations that have been made of X-ray flares during which infrared observations were carried out.

Submm-VLBI of Sgr A* with EHT- Shadow of a Black Hole

In general relativity, photons move along geodesics in a curved spacetime, leading to the bending of light rays. Therefore, the appearance of a black hole put in front of a larger bright source is expected to be a black disk with a diameter greater than the event horizon. This effect has been called the “shadow” of the black hole.

The angular radius of the shadow of a black hole is primarily determined by its mass-to-distance ratio and depends only weakly on its spin and inclination. However, if general relativity is violated, the shadow size may also depend strongly on parametric deviations from the Kerr

metric. Based on a reconstructed image of Sgr A* from a simulated one-day observing run of a seven-station Event Horizon Telescope (EHT) array, Johannsen et al. (2016) used Markov chain Monte Carlo algorithm to demonstrate that such an observation can measure the angular radius of the shadow of Sgr A* with an uncertainty of $\sim 1.5 \mu\text{as}$ (6%).

Sgr A* has been studied on Schwarzschild radius scales with (sub)millimeter wavelength Very Long Baseline Interferometry (VLBI) which offer the highest angular resolution possible today; however they suffer from interstellar scattering which broadens the radio image. Fish et. al (2011) conducted VLBI observations at 1.3 mm and used that to address two fundamental questions concerning the nature of Sgr A*. The first is whether the accretion flow surrounding Sgr A* exhibits an expected “shadow” feature that occurs due to the strong gravitational lensing near the black hole. Emission from the accretion flow is preferentially lensed onto the last photon orbit, resulting in a relatively dim central region encircled by a brighter annulus (Falcke et al. 2000). The second question they tried to answer is whether the flaring behavior exhibited by Sgr A* has its origins in compact structures that arise near the black hole event horizon. Broadband flares on timescales ranging from minutes to hours are well-documented (Marrone et al. 2008; Yusef-Zadeh et al. 2009; Dodds-Eden et al. 2009) and imply time-variable structures in the innermost accretion region. If small-scale variable structures are present, 1.3 mm VLBI can sensitively monitor the changing morphology of Sgr A* using non-imaging techniques with time resolutions of tens of seconds (Doeleman et al. 2009; Fish et al. 2009b).

“**Event Horizon Telescope**” or EHT depicts the existing and planned VLBI stations employed in Sgr A* imaging. EHT, is a radio-telescope planetary network, and its goal is to reach a

sufficiently high spatial resolution to obtain real images of Sgr A*. It should allow us to analyse predicted EHT data obtained from a simulations to "see" the event horizon and the neighborhood of Sgr A*. The final plan involves expanding the set of available sub-mm telescopes to at least 13 for the full EHT functionality.

The “no hair” theorem of the black hole physics, based on General Relativity theory, predicts that the space-time around a black hole can be expressed in terms of only three physical parameters: the mass of the black hole, its intrinsic angular moment, or spin and its electric charge, if present (Raine and Thomas, 2010).

As per General Relativity, warping of space around a black hole produces a dark shadow surrounded by a bright ring of photons. The shape of this ring is approximately circular. Ability to detect that structure of the black hole using future observations, will allow the possibility to verify the correctness of the theory. The shadow diameter of a BH is given by: $10 m$, where, $m = \frac{GM}{c^2}$ is the geometrical mass of the BH which independent of the rotation (Raine and Thomas, 2010). Figure 1.6 depicts the possible shapes of shadows in the vicinity of the BH.



Figure 1.6 – Possible shadow shapes in the neighborhood of a black hole (Broderick et. al, 2014).

General Relativistic theory predicts that the shadow of a black hole should be circular (center image), but a black hole that violates the "no hair" theorem could have a prolate shadow (left image) or oblate (right image) . Future real “Event Horizon Telescope”, EHT, images Sgr A*.

The shadow radius of Sgr A* is: $\sim 3.015 \times 10^7$ km, which at the distance of the source is equal to $\sim 5 \times 10^{-5}$ arcseconds. The radius of its event horizon is $\sim 12 \times 10^6$ km, i.e. 17 times the equatorial radius of the Sun (Raine and Thomas, 2010).

Johannsen et. al (2016) analyzed predicted EHT data obtained from a simulation to study the event horizon and the neighborhood of Sgr A* (figure 1.7). They first showed that the EHT will dramatically reduce the uncertainties in the mass and distance measurements. They also describe in detail how the EHT will test general relativity by measuring certain spacetime deviation parameters that have nonzero values in alternative gravity theories.

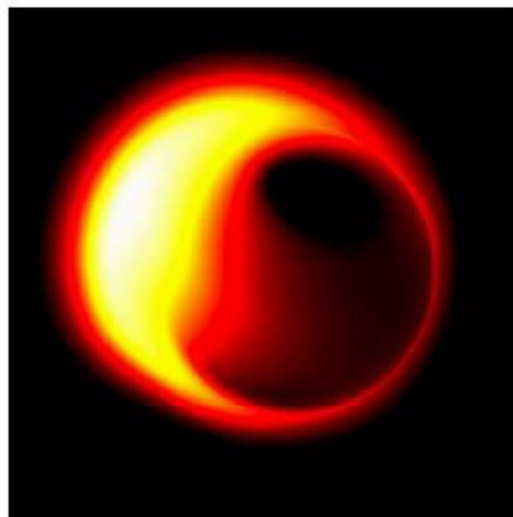


Figure 1.7 – Image simulation of the event horizon and the neighborhood of Sgr A*.
From Johannsen et al., (2016)

The dark region visible in figure 1.7 is surrounded by a light ring which are theorised to be accumulated photons. The very bright region corresponds to a peak of emission due to the matter spiralling inside the gravitational field of the supermassive BH.

Conclusion

In conclusion, Sgr A* stands out from its surrounding radio sources and is unique in several ways. Its compactness (point-like) and non-thermal spectrum are reminiscent of the compact nuclear radio sources associated with typical AGNs. The proximity of Sgr A* (8 kpc), however, offers us a unique opportunity for testing the SMBH (supermassive black hole) paradigm, which is not possible in the case of AGNs. The next closest galactic nucleus (M 31*) is ~ 100 times farther away from us than Sgr A*. As shown in Table 1, apparent angular sizes of several black hole event horizons are compared for several (notable) sources. In terms of apparent size, Sgr A* is the largest black hole candidate.

Table 1

| Source | Distance [$\times 10^6$ pc] | Mass [$\times 10^6 M_\odot$] | θ_H [μ as] | Reference |
|--------------|---------------------------------|-----------------------------------|---------------------------|-----------|
| Sgr A* | 8.0×10^{-3} | 4.0 | 10 | 1 |
| M 87 | 17.9 | 6.4×10^3 | 7 | 2 |
| M 31 | 0.77 | 56.2 | 1.4 | 3 |
| NGC 4258 | 7.2 | 36 | 0.1 | 4 |
| Stellar mass | 1×10^{-6} | 1 | 0.02 | assumed |

References: (1) Both mass and distance from Gebhardt & Thomas (2009) (2) Salow & Statler (2004) (3) References within (2); (4) mass from Miyoshi et al. (1995) and distance from Herrnstein et al. (1999). Adapted and updated from Miyoshi & Kameno (2002).

Imaging of the event horizon of Sgr A* would soon be possible (Doeleman et al. 2009a) with the Event Horizon Telescope (EHT), providing valuable insights into black hole accreting systems and the study of physics near the event horizon.

The main goal of high frequency VLBI is to directly address following four questions throughout next several years:

- Does General Relativity hold in the strong field regime?
- Is there an Event Horizon?
- Can we estimate Black Hole spin by resolving orbits near the Event Horizon?
- How do Black Holes accrete matter and create powerful jets?

References:

- Amo-Baladron, M. A., Martin-Pintado, J., Morris, M. R., Muno, M. P., & Rodr'iguez-Fern'andez, N. J. 2009, *ApJ*, 694, 943
- Baganoff, F. K., Bautz, M. W., Brandt, W. N., et al. 2001, *Nature*, 413, 45
- Baganoff, F. K., Maeda, Y., Morris, M., et al. 2003, *ApJ*, 591, 891
- Bardeen, J.M. 1974, in *IAU Symposium*, 64, *Gravitational Radiation and Gravitational Collapse*, ed. C. Dewitt-Morette, 132
- Bardeen, J. M., Press, W. H., & Teukolsky, S. A. 1972, *ApJ*, 178, 347
- Bartko, H., Martins, F., Fritz, T. K., et al. 2009, *ApJ*, 697, 1741
- Becklin, E. E., & Neugebauer, G. 1968, *ApJ*, 151, 145
- Bower, G. C., Falcke, H., Sault, R. J., & Backer, D. C. 2002, *ApJ*, 571, 843
- Bower, G. C., Falcke, H., Herrnstein, R. M., et al. 2004, *Science*, 304, 704
- Bower, G. C., Goss, W. M., Falcke, H., Backer, D. C., & Lithwick, Y. 2006, *ApJ*, 648, L127
- Broderick, A. E., & Narayan, R. 2006, *ApJ*, 638, L21
- Broderick, A. E., Loeb, A., & Narayan, R. 2009a, *ApJ*, 701, 1357
- Broderick, A. E., Fish, V. L., Doeleman, S. S., & Loeb, A. 2009b, *ApJ*, 697, 45
- Broderick, A. E., Johannsen, T., Loeb, A., Psaltis, D. 2014, *Astrophys. J.*, 784, 7

- Burkert, A., Schartmann, M., Alig, C., et al. 2012, *ApJ*, 750, 58
- Chan, C.-K., Liu, S., Fryer, C. L., Psaltis, D., Ozel, F., Rockefeller, G. and Melia, F. 2009, *ApJ*, 701, 521
- Do, T., Ghez, A. M., Morris, M. R., et al. 2009, *ApJ*, 691, 1021
- Dodds-Eden, K., Porquet, D., Trap, G., et al. 2009, *ApJ*, 698, 676
- Dodds-Eden, K., Gillessen, S., Fritz, T. K., et al. 2011, *ApJ*, 728, 37
- Doeleman, S. S., Weintroub, J., Rogers, A. E. E., et al. 2008, *Nature*, 455, 78
- Eckart, A., Genzel, R., Ott, T., & Schödel, R. 2002, *MNRAS*, 331, 917
- Eckart, A., Baganoff, F. K., Morris, M., et al. 2004, *A&A*, 427, 1
- Eckart, A., Baganoff, F. K., Schödel, R., et al. 2006a, *A&A*, 450, 535
- Eckart, A., Schödel, R., Meyer, L., et al. 2006b, *A&A*, 455, 1
- Eckart, A., Schödel, R., Garcia-Marin, M., et al. 2008, *A&A*, 492, 337
- Eckart, A., Baganoff, F. K., Morris, M. R., et al. 2009, *A&A*, 500, 935
- Eckart, A., Garcia-Marin, M., Vogel, S. N., et al. 2012, *A&A*, 537, A52
- EHT, http://www.eventhorizontelescope.org/science/general_relativity.html
- Falcke, H., Melia, F., & Agol, E. 2000, *ApJ*, 528, L13
- Fish, V. L., Doeleman, S. S., Beaudoin, C., et al. 2011. 1.3 mm wavelength VLBI of Sagittarius A*: Detection of time-variable emission on event horizon scales. *ApJL*, 727, L36{L41
- Gebhardt, K., & Thomas, J. 2009, *ApJ*, 700, 1690
- Genzel, R., Schödel, R., Ott, T., et al. 2003, *Nature*, 425, 934
- Genzel, R., Eisenhauer, F., & Gillessen, S. 2010, *Reviews of Modern Physics*, 82, 3121
- Ghez, A. M., Klein, B. L., Morris, M., & Becklin, E. E. 1998, *ApJ*, 509, 678
- Ghez, A. M., Morris, M., Becklin, E. E., Tanner, A., & Kremenek, T. 2000, *Nature*, 407, 349
- Ghez, A. M., Duchene, G., Matthews, K., et al. 2003, *ApJ*, 586, L127
- Ghez, A. M., Wright, S. A., Matthews, K., et al. 2004, *ApJ*, 601, L159
- Ghez, A. M., Salim, S., Hornstein, S. D., et al. 2005a, *ApJ*, 620, 744
- Ghez, A. M., Hornstein, S. D., Lu, J. R., et al. 2005b, *ApJ*, 635, 1087
- Ghez, A. M., Salim, S., Weinberg, N. N., et al. 2008, *ApJ*, 689, 1044
- Gillessen, S., Genzel, R., Fritz, T. K., et al. 2012, *Nature*, 481, 51
- Johannsen, T., et al. 2016, Testing General Relativity with the Shadow Size of Sgr A*, *PRL* 116, 031101

- Macquart, J. P., & Bower, G. C. 2006, *ApJ*, 641, 302
- Marrone, D. P., Moran, J. M., Zhao, J.-H., & Rao, R. 2006, *ApJ*, 640, 308
- Marrone, D. P., Baganoff, F. K., Morris, M. R., et al. 2008, *ApJ*, 682, 373
- Martin-Pintado, J., de Vicente, P., Rodr'iguez-Fernandez, N. J., Fuente, A., & Planesas, P. 2000, *A&A*, 356, L5
- Mauerhan, J. C., Morris, M., Walter, F., & Baganoff, F. K. 2005, *ApJ*, 623, L25
- McHardy, I. M., Koerding, E., Knigge, C., Uttley, P., & Fender, R. P. 2006, *Nature*, 444, 730
- Melia, F., & Falcke, H. 2001, *ARA&A*, 39, 309
- Meyer, L., Ghez, A. M., Schödel, R., et al. 2012. The shortest-known-period star orbiting our Galaxy's supermassive black hole. *Science*, 338, 84-87
- Meyer, L., Schödel, R., Eckart, A., et al. 2006a, *A&A*, 458, L25
- Meyer, L., Eckart, A., Schödel, R., et al. 2006b, *A&A*, 460, 15
- Meyer, L., Schödel, R., Eckart, A., et al. 2007, *A&A*, 473, 707
- Meyer, L., Do, T., Ghez, A., et al. 2008, *ApJ*, 688, L17
- Meyer, L., Do, T., Ghez, A., et al. 2009, *ApJ*, 694, L87
- Miyoshi, M., & Kamenno, S. 2002, in *International VLBI Service for Geodesy and Astrometry General Meeting Proceeding*, p. 199, 199
- Miyoshi, M., Moran, J., Herrnstein, J., et al. 1995, *Nature*, 373, 127
- Morris, M. 2012, *Nature*, 481, 32
- Morris, M. R., Wang, Q. D., & Yuan, F., eds. 2011, in *Astronomical Society of the Pacific Conference Series*, 439, *The Galactic Center: a Window to the Nuclear Environment of Disk Galaxies*
- Morris, M. R., Meyer, L., Ghez, A., 2012, *Research in Astron. Astrophys.*, Vol. 12, No. 8, 995–1020
- Nobukawa, M., Ryu, S. G., Tsuru, T. G., & Koyama, K. 2011, *ApJ*, 739, L52
- Nowak, M.A., Neilsen, J., Markoff, S.B., Baganoff, F.K. et al. 2012, *ApJ*, preprint
- Odaka, H., Aharonian, F., Watanabe, S., et al. 2011, *ApJ*, 740, 103
- Porquet, D., Predehl, P., Aschenbach, B., et al. 2003, *A&A*, 407, L17
- Porquet, D., Grosso, N., Predehl, P., et al. 2008, *A&A*, 488, 549
- Raine, D. & Thomas, E. 2010, *Black Holes, An Introduction*, 2nd ed., Imperial College Press

- Rauch, C.; Ros, E.; Krichbaum, T. P.; Eckart, A.; et al 2016, *Astronomy and Astrophysics*, 587
- Reid, M. J., Menten, K. M., Zheng, X. W., Brunthaler, A., & Xu, Y. 2009, *ApJ*, 705, 1548
- Reid, M. J. and Brunthaler, A. 2004. The proper motion of Sagittarius A*. II. The mass of Sagittarius A*, *ApJ*, 616, 872-884
- Rodriguez-Fernandez, N. J., Martín-Pintado, J., Fuente, A., & Wilson, T. L. 2004, *A&A*, 427, 217
- Russell, D. M., Gallo, E. and Fender, R. P. 2013. Observational constraints on the powering mechanism of transient relativistic jets. *MNRAS*, 431, 405-414.
- Salow, R. M., & Statler, T. S. 2004, *ApJ*, 611, 245
- Schartmann, M., Burkert, A., Alig, C., et al. 2012, *arXiv:1203.6356*
- Schödel, R., Ott, T., Genzel, R., et al. 2002, *Nature*, 419, 694
- Shcherbakov, R. V., & Baganoff, F. K. 2010, *ApJ*, 716, 504
- Uttley, P., & McHardy, I. M. 2005, *MNRAS*, 363, 586
- Witzel, G., Eckart, A., & Bremer, M. et al. 2012, *ApJS*, 203, 18
- Yusef-Zadeh, F., Law, C., & Wardle, M. 2002, *ApJ*, 568, L121
- Yusef-Zadeh, F., Bushouse, H., Dowell, C. D., et al. 2006a, *ApJ*, 644, 198
- Yusef-Zadeh, F., Roberts, D., Wardle, M., Heinke, C. O., & Bower, G. C. 2006b, *ApJ*, 650, 189
- Yusef-Zadeh, F., Munro, M., Wardle, M., & Lis, D. C. 2007, *ApJ*, 656, 847
- Yusef-Zadeh, F., Wardle, M., Heinke, C., et al. 2008, *ApJ*, 682, 361
- Yusef-Zadeh, F., Bushouse, H., Wardle, M., et al. 2009, *ApJ*, 706, 348
- Yusef-Zadeh, F., Wardle, M., Dodds-Eden, K., et al. 2012, *AJ*, 144, 1
- Zajaček M., et al., 2017, preprint, (*arXiv:1704.03699*)
- Zamaninasab, M., Eckart, A., Witzel, G., et al. 2010, *A&A*, 510, A3
- Zhao, J., Ekers, R. D., Goss, W. M., Lo, K. Y., & Narayan, R. 1989, in *IAU Symposium*, 136, The Center of the Galaxy, ed. M. Morris (Dordrecht: Kluwer), 535
- Zhao, J.-H., Young, K. H., Herrnstein, R. M., et al. 2003, *ApJ*, 586, L29
- Zhao, J.-H., Morris, M. R., Goss, W. M., & An, T. 2009, *ApJ*, 699, 186
- Zucker, S., Alexander, T., Gillessen, S., Eisenhauer, F., & Genzel, R. 2006, *ApJ*, 639, L21